Artificial Intelligence for Engineering Design, Analysis and Manufacturing

cambridge.org/aie

Developing a new hybrid soft computing technique in predicting ultimate pile bearing capacity using cone penetration test data

Hooman Harandizadeh

Department of Civil Engineering, Faculty of Engineering, Shahid Bahonar University of Kerman, Pajoohesh Sq., Imam Khomeni Highway, Post Office Box: 76169133, Kerman 7616913439, Iran

Research Article

Cite this article: Harandizadeh H (2020). Developing a new hybrid soft computing technique in predicting ultimate pile bearing capacity using cone penetration test data. *Artificial Intelligence for Engineering Design, Analysis and Manufacturing* **34**, 114–126. https://doi.org/10.1017/S0890060420000025

Received: 24 March 2019
Revised: 29 November 2019
Accepted: 7 December 2019
First published online: 30 January 2020

Key words:
ANFIS algorithm; CPT-based models; GMDH type neural network; pile bearing capacity; PSO algorithm

Author for correspondence: Hooman Harandizadeh, E-mail: hoomanharandizadeh@eng.uk.ac.ir

Abstract

This research intends to investigate a new hybrid artificial intelligence (AI) technique compared to some common CPT methods in estimating axial ultimate pile bearing capacity (UPBC) using cone penetration test (CPT) data in geotechnical engineering applications. A data series of 108 samples was collected in order to develop a new hybrid structure of an adaptive neuro-fuzzy inference system (ANFIS) network, and the group method of the data handling (GMDH) type neural network was optimized by applying the particle swarm optimization (PSO) algorithm over the hybrid ANFIS-GMDH topology, which leads to a new hybrid AI model called as ANFIS-GMDH-PSO. The derived database provides information related to pile load tests, *in situ* field CPT data, and soil–pile information for introducing the proposed hybrid neural system. The cross-section of the pile toe, average cone tip resistance along embedded pile length, and sleeve frictional resistance along the shaft had been considered as input parameters for the proposed network. The results of this research indicated that the proposed ANFIS-GMDH-PSO model predicted the UPBC with an acceptable precision compared to various CPT methods, including Schmertmann, De Kuiter & Bringen, and LPC/LPCT methods. Moreover, ANFIS-GMDH-PSO network model performance was compared to CPT-based models in terms of statistical criteria in order to achieve a best fitted model. From the statistical results, it was found that the developed ANFIS-GMDH-PSO model has achieved a higher accuracy level in terms of statistical indices compared to CPT-based empirical methods, such as Schmertmann model, De Kuiter & Beringen model, and Bustamante & Gianeselli for predicting driven pile ultimate bearing capacity.

Introduction

Deep structural foundations (piles) are applied in positions in which the underneath layers of the soil are not capable of bearing the applied structural loads only by foundations. The main reason for applying deep foundation is to transmit the structural applied loads into the stiff denser soil layers in order that they have features to carry structural loads. Therefore, stability and safety of superstructures located on shallow foundations will depend on the pile's behavior. In order to guarantee the stability analysis of shallow foundations, it is very important to attain an exact approximation of axial pile capacity in the soil, especially for design purposes. This problem has become one of the challenging issues in geotechnical engineering since unseen influence parameters and uncertainties affect soil and pile interaction, for instance, the complex behavior of the pile within soil environments, soil disturbing caused by the pile setup and sampling methods, and the load transferring mechanism in the pile (Kiefa, 1998).

Based on the load transferring characteristics to the underneath layer, the total axial ultimate pile capacity (Q_u) generally determines the sum of the pile tip load bearing capacity (Q_t) (i.e., dense layers/stiff layers bearing capacity through which applied loads are transmitted onto), and bearing capacity of shaft (Q_s) (i.e., bearing capacity transferred through surrounding the friction soil over pile shaft axis) (Niazi and Mayne, 2013), which is stated by

$$Q_u = Q_t + Q_s = q_t \cdot A_t + \sum_{i=1}^{n} f_{s(i)} \cdot A_{si}, \quad (1)$$

where q_t is the tip bearing capacity, A_t is the pile toe cross-section area, f_s is the unit resistance of the shaft within the ith layer of the soil profile in which the pile shaft length is embedded; A_{si} is the contact area that provides shaft frictional resistance with the surrounding soil in the ith layer. The most common methods employed to calculate ultimate axial pile capacity could be categorized into subsequent groups: (1) pile loading tests (PLT), (2) semi-empirical and analytical approaches, and (3) CPT- and SPT-based methods associated with *in situ* field tests.

© Cambridge University Press 2020

CAMBRIDGE UNIVERSITY PRESS

Carrying out the PLT method is often time-consuming and expensive in most cases; these tests require advanced equipment with a professional specialist. In addition, most analytical methods often use a number of simplifying assumptions to calculate the load bearing capacity, which encounters many errors. Consequently, some correlations have been proposed by previous researchers to establish a relation between ultimate pile bearing capacity (UPBC) and *in situ* tests results (Niazi and Mayne, 2013). Among some *in situ* experiments, the cone penetration test (CPT) is considered as the most effective method for describing the soil properties at various depths. In addition, CPT is a commonly used soil exploration survey in engineering applications because it is quick, economic, and could continuously obtain physical soil parameters (Eslami, 1997; Abu-Farsakh and Titi, 2004). In recent years, some researchers developed concepts of advanced artificial intelligence (AI) in different engineering applications, such as engineering mechanics, design of energy-saving buildings, automation, and construction (Coello and Aguirre, 2002; Nariman-Zadeh *et al.*, 2003; Hanna, 2007; Padmini *et al.*, 2008; Rossi and Lanzetta, 2013; Hu *et al.*, 2014; Zeng *et al.*, 2014; Kontovourkis *et al.*, 2015; Salido *et al.*, 2015; Adeniran and El-Ferik, 2017; Persson and Ölvander, 2017; Thimmisetty *et al.*, 2017; Al-Refaie *et al.*, 2018; Keles, 2018; Lin and Huang, 2018; Mirabi and Seddighi, 2018; Zimmermann *et al.*, 2018). In recent years, applications of AI models have become widespread through civil engineering projects (e.g., Armaghani *et al.*, 2017, 2018; Koopialipoor *et al.*, 2018). In this way, a large number of experts in the field of geotechnical engineering (Shahin, 2010) have made rigorous efforts to employ various AI approaches to establish general traditional equation-based evolutionary computing so as to obtain a more accurate prediction bearing capacity of piles rather than conventional models based on CPT databases (Momeni *et al.*, 2014, 2015, 2018). In the case of pile bearing capacity prediction, several research works were conducted to predict pile bearing capacity by using quite a few data-driven models, such as hybrid artificial neural networks (ANN-PSO, ANN-GA and ANN-ICA), support vector machine (SVM), and gene-expression programming (GEP) (e.g., Abu-Kiefa, 1998; Alkroosh and Nikraz, 2011, 2012; Momeni *et al.*, 2014; Faizi *et al.*, 2015; Ebrahimian and Movahed, 2016; Moayedi and Armaghani 2018) . Among these AI models, previous investigations have proved that the GMDH network is comparatively more flexible than other AI techniques, such as ANNs and ANFIS (e.g., Najafzadeh et al., 2013a, 2013b, 2018; Shaghaghi *et al.*, 2017; Harandizadeh *et al.*, 2018). More importantly, there are a few applications of GMDH networks into geotechnical engineering which indicated this model can be employed successfully in some investigations such as mechanical properties of soils (Kalantary *et al.*, 2009)), assessment of tunnel boring machine (Koopialipoor *et al.*, 2018), prediction of soil shear strength in the drained conditions (Mola-Abasi and Eslami, 2018), and evaluation of elasticity modulus of clayed deposits (Naeinia *et al.*, 2018). Recently, Harandizadeh *et al.* (2018) have employed an improved ANFIS-GMDH model, as a feed-forward network, to obtain an accurate prediction of UPBC. Through their research work, they have developed and combined structure of the ANFIS algorithm with the GMDH algorithm in order to enhance the accuracy level of the ANFIS model; moreover, they optimized the general structure of the ANFIS-GMDH using the gravitational search algorithm (GSA). Hence, this is the second attempt to estimate UPBC by the GMDH. There is no disguising the fact that the application of the GMDH network in the estimation of UPBC has not been fully understood yet. This research subject needs still further efforts to evaluate performance of various hybrid GMDH models. In this way, the crucial aim of this research is to investigate the axial pile bearing capacity prediction using an improved GMDH model by the ANFIS technique whose general structure is optimized by means of particle swarm optimization (PSO). Furthermore, the result of the ANFIS-GMDH model is compared with those yielded by empirical equation CPT-based models.

Basic concepts of CPT-based methods

Schmertmann CPT method

In recent decades, various direct and indirect *in situ* CPTs were established for subsurface exploration and estimating soil strength parameters (ϕ and c) as well as pile capacity prediction; the Schmertmann method was developed based on 108 experimental pile load test (PLTs) results performed on different ranges of piles by Nottingham (Schmertmann, 1978) in order to calculate ultimate piles bearing capacity; based on this method, the ultimate pile tip resistance capacity Q_P was derived by

$$Q_p = \left(\frac{q_{c1} + q_{c2}}{2}\right) \cdot A_{tip}, \tag{2}$$

where A_{tip} is the pile tip cross-section, q_{c1} and q_{c2} indicate the – average pile tip resistance in the range of 0.74D beneath the pile toe region, and in the range of 8D above the pile toe region, respectively (Schmertmann, 1978). The average resistance of the cone tip is derived from the representation of the failure surface presumed to trace the logarithmic shape as presented by Begemann (1963). This method bounds q_{c1} and q_{c2} values to 15 MPa. According to the Schmertmann ethod (Schmertmann, 1978), the skin friction resistance is expressed by Eqs (3) and (4), respectively, for clayey and sandy soils:

$$Q_s = \alpha_c f_s A_s \quad \text{in clay}, \tag{3}$$

$$Q_s = \alpha_s \left[\sum_{d=0}^{8D} \frac{1}{2} f_s A_s + \sum_{d=8D}^{L} f_s A_s\right] \quad \text{in sand}, \tag{4}$$

where D and A_s denote the equivalent pile diameter or pile width and soil–pile contact area, respectively; α_c and α_s denote resistance of the shaft to the sleeve friction ratio for clayey and sandy soils; α_c values vary from range of 0.2 to 1.2 and is a function of sleeve friction values while α_s values depend on pile embedded length to equivalent diameter of pile ratio varying from 0.4 to 4 values. f_s denotes the average friction of the shaft sleeve.

De Kuiter and Beringen CPT method

After Schmertmann, another effective CPT predictive method was extended by De Kuiter and Bringen (1979) based on experimental results carried in some regions of the North ocean. They indicated that in clayey soil, the unit pile toe resistance and shaft resistance capacity were identified from the undrained soil shear strength

https://doi.org/10.1017/S0890060420000025 Published online by Cambridge University Press

Table 1. Statistical variables description used in the developed ANFIS-GMDH-PSO model

Parameter	A_t (cm^2)	A_s (m^2)	$\bar{q}_{c-shaft}$ (MPa)	$\bar{f}_s$ (KN)	$\bar{q}_{c-tip}$ (MPa)	P_u (KN)
Mean	1736	26.46	5.84	101.89	8.82	1965.86
Median	1228	17.78	5.34	80.02	7.63	1340
Mode	950	11.12	6.57	73	20	1140
Standard deviation	1674	26.17	4.45	65.4	6.19	1702.20
Minimum	20	5.45	0.833	9.39	0.25	60
Maximum	7854	194.65	24.707	349.64	27.11	10,910
Count	108	108	108	108	108	108

based on Eqs (5) and (6), respectively.

$$\text{The unit pile tip resistance in clay soils}: q_p = N_c S_u, \quad (5)$$

$$\text{The unit shaft resistance in clay soils}: f = \alpha' S_u, \quad (6)$$

where α' denoting the cohesion factor is taken in (OC) clay to be equal to 0.5, and for (NC) clay equal to 1; N_c denotes the bearing capacity coefficient and S_u demonstrates the undrained shear strength which is derived from

$$S_u = \frac{q_{ca}}{N_k}, \quad (7)$$

in which N_k– denotes the cone coefficient varying within the range of 520; in addition, according to this method, the unit skin frictional resistance in the sand was defined through

$$f = \min\{f_s, q_c/300, 120\,\text{kPa},\} \quad (8)$$

where q_c and f_s are the unit resistance of the cone tip and unit sleeve friction, respectively.

Similarly, they observed that the pile toe resistance capacity in the sand was found to be the same as that obtained by the Schmertmann method procedure (Schmertmann, 1978).

Bustamante and Gianeselli CPT method (LPC/LPCT)

The proposed LPC method was conducted by Bustamante and Gianeselli (1982) carrying out some experimental tests on piles for developing a French highway project. In this approach, the unit pile toe resistance and unit pile shaft resistance are stimulated from cone tip resistance by ignoring the sleeves friction. The unit resistance of the pile tip is estimated using the following equation:

$$q_p = k_b q_{ca}, \quad (9)$$

in which q_{ca} is the average value of q_c over the influence zone ranging from 1.5D (pile diameter) below and above of the pile toe region, and k_b is a coefficient dependent on soil properties and the pile setup method. The unit shaft resistance capacity was established using the following equation:

$$f = \frac{q_c}{k_s}, \quad (10)$$

in which q_c is the mean resistance of the cone tip along the pile length and k_s is a coefficient depending on pile materials and setup methods.

Materials

A proposed ANFIS-GMDH-PSO model was developed based on 108 data sets derived from the literature. In the developed model, the cluster parameters and ANFIS membership functions were improved and adjusted by applying the PSO technique. This section discussed data source details and effective input variables presented by the hybrid ANFIS-GMDH-PSO model. A database consists of 108 samples derived from previous research (Eslami, 1997; Nejad *et al.*, 2009).

The Dara source covers various variables including static PLT (ML or CRP), pile materials (steel, concrete, composite), pile set-up method (drilled or driven), and pile end type (open or closed); the effective input variables are taken into account as the pile tip cross-section A_t, A_s is the sleeve shaft cross-section, the average resistance of cone tip value along shaft length $\bar{q}_{c-shaft}$, and the average resistance of the cone tip value over pile tip influence zone $\bar{q}_{c-tip}$.

The measured ultimate bearing capacity P_u is derived from full-scale static pile loading test results. For piles that failed during the test, the failure load was considered as the UPBC; for other piles, 80% failure criteria proposed by Hansen was used (Kondner, 1963). The ANFIS-GMDH-PSO model output is the axial pile load bearing capacity (P_u) expressed as a function of effective input parameters in general form by

$$P_u = f(A_t, A_s, \bar{q}_{c-shaft}, \bar{q}_{c-tip}, \bar{f}_s). \quad (11)$$

The under-study parameter description used to develop the model is summarized in Table 1.

Methodology

The research methodology is explained in subsequent sections; first, a brief description of different AI methods was described in detail including ANFIS [Description of adaptive neuro-fuzzy inference system (ANFIS)], GMDH type neural network structures (Description of GMDH type neural network framework), and PSO algorithm (Description of PSO framework); then the hybridization process of the ANFIS-GMDH network structure was explained (Development of hybrid ANFIS-GMDH structure) and finally the developed ANFIS-GMDH model was optimized

https://doi.org/10.1017/S0890060420000025 Published online by Cambridge University Press

based on the PSO algorithm over the hybrid ANFIS-GMDH topology structure (Development of hybrid ANFIS-GMDH-PSO algorithm).

Description of ANFIS

The ANFIS structure used in this study is shown in Figure 3 (Zhang et al. 2006). The rules of the fuzzy inference system applied in the ANFIS network structure are demonstrated based on Takagi–Sugeno–Kang' approach that utilizes membership functions instead of using fuzzy sets theory applied through the fuzzy inference system of Mamdani's approach (Zadeh, 1996). For simplicity, a fuzzy inference rule of R^r applying the first-order TSK method (Takagi and Sugeno, 1993) could be expressed by

$$R^r: \text{ If } x_1 \text{ is } A_{1j} \text{ AND } \ldots \text{ AND } x_n \text{ is } A_{nj} \text{ then } \widehat{y} \text{ is } w_r \qquad (12)$$

in which x_i indicates the ith input variable of the neuro-fuzzy system (n represents the input variables number), A_{ij} denotes the jth membership function of antecedent part of the input variable x_i ($j = 1, 2, \ldots, K_i$), K_i expresses the number of fuzzy sets for each input variable x_i, and w_r are the consequent part parameters ($r = 1, 2, \ldots, R$), $\widehat{y}$ is single output, and $R = \prod_{i=1}^{n} K_i$ is fuzzy rules number (number of rules) made by taking into account all fuzzy sets combination. The ANFIS network consisted of four different layers described briefly below. *Layer 1 (Layer of input):* Through passing this layer, the x_i values are entered into the second layer without any changes.

Layer 2 (Layer of fuzzification): Through the nodes of this layer, the Gaussian-type arbitrary membership functions are defined with σ_{ij} (standard deviation) and c_{ij} (center) for x_i (input variable) by

$$A_{ij}(x_i) = \exp - \frac{(x_i - c_{ij})^2}{\sigma_{ij}^2}, j = 1, \ldots, K_i. \qquad (13)$$

Layer 3 (Layer of inference): The nodes within this layer generate an antecedent part of the fuzzy rule using fuzzy AND/OR operators to obtain the firing strength of F_r extracted from the fuzzy rule of the rth based on membership functions values using the following equation:

$$F_r = \prod_{i=1}^{n} A_{ij}(x_i), r = 1, 2, \ldots, R \text{ and } j = 1, 2, \ldots, K_i \qquad (14)$$

Layer 4 (Layer of output): This layer is composed of a single node denoted as the final ANFIS output. The estimated output for the ANFIS is described below in Eq. (15):

$$\widehat{y} = \sum_{r=1}^{R} F_r w_r \qquad (15)$$

Description of the GMDH type neural network framework

The idea associated with ANNs stimulated through the modeling structure of the complex human brain is known as a non-linear, parallel performing approach (Haykin et al., 1999). The GMDH type neural network structure is the self-organizing method by which a behavior system is identified by the assessment of its

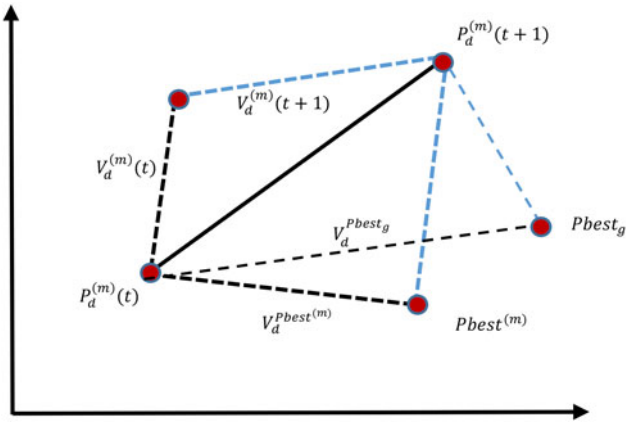


Fig. 1. PSO search mechanism.

performances over a provided set of multi-input single output data set (x_i, x_j), ($i = 1, 2, \ldots, M$). The concept of the GMDH network is to make an analytic function within a feed-forward network determined by a polynomial transfer function in which coefficients are attained by applying the particular regression process (Najafzadeh *et al.*, 2013). By applying the GMDH algorithm, a model is displayed as a set of neurons through which various sets in every single layer are usually interconnected through a quadratic polynomial, creating new neurons inside the subsequent layer. These types of representation is employed to map input space to output space (Najafzadeh and Azamathulla, 2013; Najafzadeh *et al.*, 2014; Najafzadeh, 2015). The basic description of the identification issue is to uncover a function ($\hat{f}$) utilized as opposed to the desired function (f) as a way to predict the output result ($\hat{y}$) for any provided input vector $X = (x_1, x_2, x_3, \ldots, x_n)$ as close as possible toward the target value (y). For that reason, M observations involving multivariable input–single variable output data set are established by Eq. (16) (Najafzadeh and Barani, 2011; Najafzadeh and Azamathulla, 2013; Najafzadeh and Lim, 2015):

$$y_i = f(x_{i1}, x_{i2}, x_{i3}, \ldots, x_{in}), (i = 1, 2, 3, \ldots M). \qquad (16)$$

It could be practical to train a GMDH type of the artificial neural network to estimate predicted values ($\hat{y}_i$) considered to be for each provided input vector *(X)*:

$$\hat{y}_i = \hat{f}(x_{i1}, x_{i2}, x_{i3}, \ldots, x_{in}) \ (i = 1, 2, 3, \ldots, M). \qquad (17)$$

The main issue is to specify a GMDH type neural network to ensure square of the differences between observed and expected output values minimized as follows:

$$\sum_{i=1}^{M} [\hat{f}(x_{i1}, x_{i2}, x_{i3}, \ldots, x_{in}) - y_i]^2 \Rightarrow \min. \qquad (18)$$

An elaborate discrete type of the Volterra functional series, referred to as Kolmogorov–Gabor polynomial, can present the general relationship among input and output parameters

https://doi.org/10.1017/S0890060420000025 Published online by Cambridge University Press

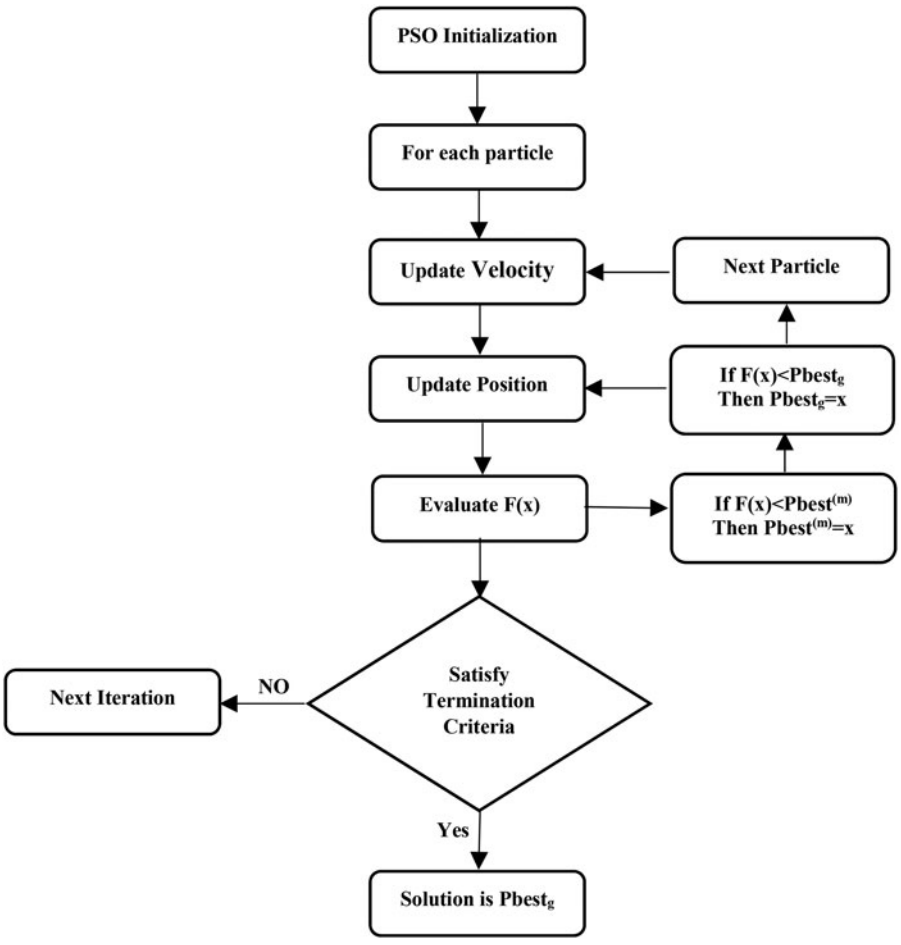


Fig. 2. Flowchart of the PSO algorithm.

mapping. As a result,

$$y = a_0 + \sum_{i=1}^{n} a_i x_i + \sum_{i=1}^{n}\sum_{j=1}^{n} a_{ij} x_i x_j + \sum_{i=1}^{n}\sum_{j=1}^{n}\sum_{k=1}^{n} a_{ijk} x_i x_j x_k + \ldots. \tag{19}$$

This specific full form of mathematical description is typically exhibited by using a solution of partial quadratic polynomials made from simply two variables (neurons) by applying

$$\hat{y} = G(x_i, x_j) = a_0 + a_1 x_i + a_2 x_j + a_3 x_i x_j + a_4 x_i^2 + a_5 x_j^2. \tag{20}$$

By using this approach, the description of a partial quadratic is recursively applied to the interconnected neurons network to develop the standard mathematical relation concerning input and output provided in Eq. (19). The a_i coefficients in Eq. (20) are computed by applying the regression method to decrease the main difference between observed output values (y) and predicted the output ones ($\hat{y}$) for each pair of input parameters (x_i, x_j). Clearly, a tree of polynomials is developed by utilizing the quadratic type provided in Eq. (20) whose coefficients are achieved by the least-square method (Najafzadeh *et al.*, 2013; Najafzadeh and Saberi-Movahed, 2019). The coefficients of each quadratic function G_i are obtained for an optimum fitting for that output associated with the total pairs of input–output data sets based on minimizing Eq. (21) criteria:

$$E = \frac{\sum_{i=1}^{M} (y_i - G_i(x_i, x_j))^2}{M} \Rightarrow \min. \tag{21}$$

For the standard form of the GMDH-type neural network formula, all possibilities of two independent variables from the total n input variables are taken into account to construct the regression polynomial by using Eq. (20) that most closely fits the dependent observations (y_i, $i = 1, 2, \ldots, M$) based on the least-squares perspective.

Therefore, $\binom{n}{2} = (n(n-2)/2)$ neurons are established within the first hidden layer from the feed-forward network using the observations $\{(y_i, x_{ip}, x_{iq}); (i = 1, 2, 3, \ldots, M)\}$ using $p, q \in \{1, 2, 3, \ldots, n\}$ in the form

$$\begin{bmatrix} x_{1p} & x_{1q} & \vdots & y_1 \\ x_{2p} & x_{2q} & \vdots & y_2 \\ \cdots & \cdots & \cdots & \cdots \\ x_{Mp} & x_{Mq} & \vdots & y_M \end{bmatrix}. \tag{22}$$

From the quadratic sub-expression, using Eq. (20) per each row of M data triples, the below matrix formulation is achieved through

https://doi.org/10.1017/S0890060420000025 Published online by Cambridge University Press

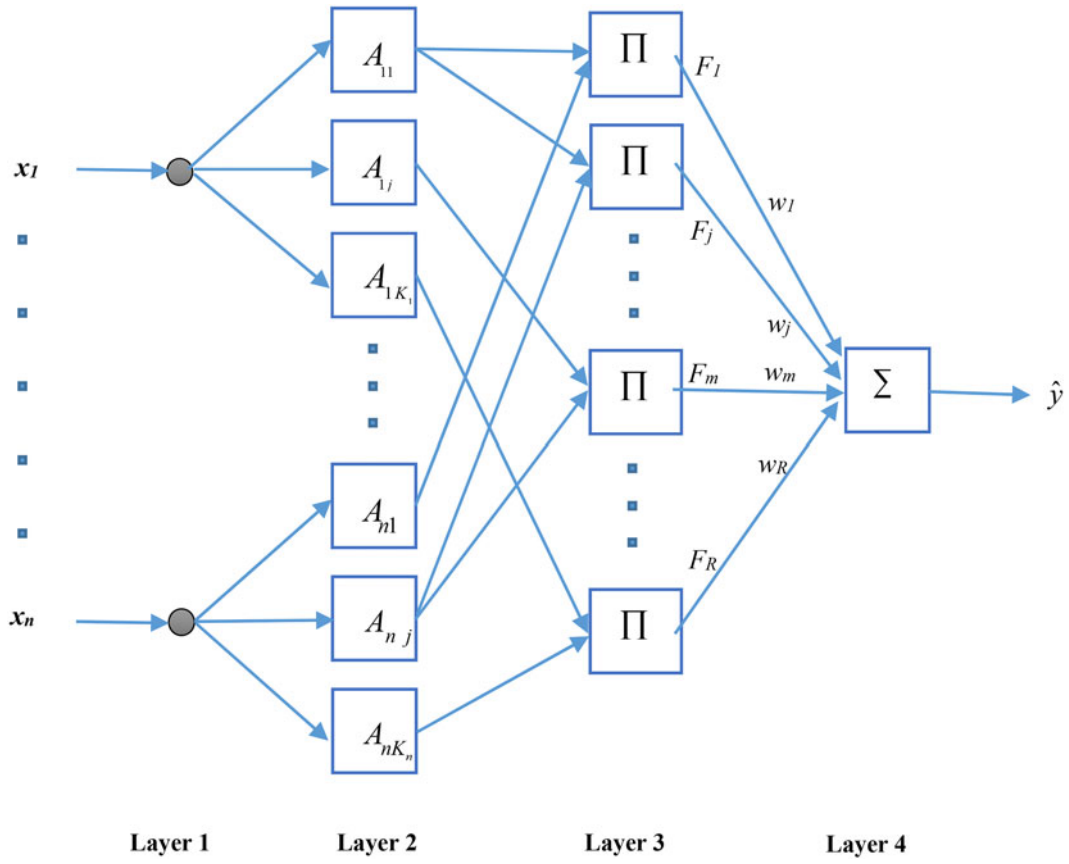


Fig. 3. ANFIS network structure.

Eqs (23)–(26), respectively:

$$Aa = Y, \tag{23}$$

$$a = \{a_0, a_1, a_2, a_3, a_4, a_5\}, \tag{24}$$

$$Y = \{y_1, y_2, y_3, \ldots, y_M\}^T, \tag{25}$$

$$A = \begin{bmatrix} 1 & x_{1p} & x_{1q} & x_{1p}x_{1q} & x_{1p}^2 & x_{1q}^2 \\ 1 & x_{2p} & x_{2q} & x_{2p}x_{2q} & x_{2p}^2 & x_{2q}^2 \\ \cdots & \cdots & \cdots & \cdots & \cdots & \cdots \\ 1 & x_{Mp} & x_{Mq} & x_{Mp}x_{Mq} & x_{Mp}^2 & x_{Mq}^2 \end{bmatrix}. \tag{26}$$

The least-squares technique from the multiple regression analysis leads to a solution of the characteristic equations in the following form:

$$a = (A^T A)^{-1} A^T Y. \tag{27}$$

The solution determines the coefficient vector of Eq. (20) for all range of M data set triples. It is observed that this process is repeated for every neuron of any succeeding hidden layer as outlined by the interconnection topology in this network (Najafzadeh and Tafarojnoruz, 2016; Najafzadeh *et al.*, 2018; Najafzadeh and Saberi-Movahed, 2019).

Development of the hybrid ANFIS-GMDH structure

In this part, the new structure of the GMDH type neural network was discussed in which partial descriptions (PDs) are ANFIS networks having two inputs in place of the RBF structure. Each PD is an ANFIS network with two inputs in which the number selection of membership functions per each input is changeable. Accordingly, the output of each PD is defined as given in Eq. (28) and Eq. (29):

$$F^{\text{pm}} = \frac{\sum_l^n \sum_k^n \mu_{A_l}(x_1^{\text{pm}})\, \mu_{B_k}(x_2^{\text{pm}}) f_{\text{lk}}^{\text{pm}}}{\sum_l^n \sum_k^n \mu_{A_l}(x_1^{\text{pm}})\, \mu_{B_k}(x_2^{\text{pm}})}, \tag{28}$$

$$f_{\text{lk}}^{\text{pm}} = q_{\text{lk}}^1 x_1 + q_{\text{lk}}^2 x_2 + q_{\text{lk}}^3, \tag{29}$$

in which m is PD number in the pth layer, n is the selected number of membership functions intended for inputs, and q coefficients are real numbers. In this case, the network output is achieved based on

$$y = \frac{1}{M} \sum_{m=1}^{M} F^{\text{pm}}. \tag{30}$$

The notation M refers to the number of PDs in the last layer.

https://doi.org/10.1017/S0890060420000025 Published online by Cambridge University Press

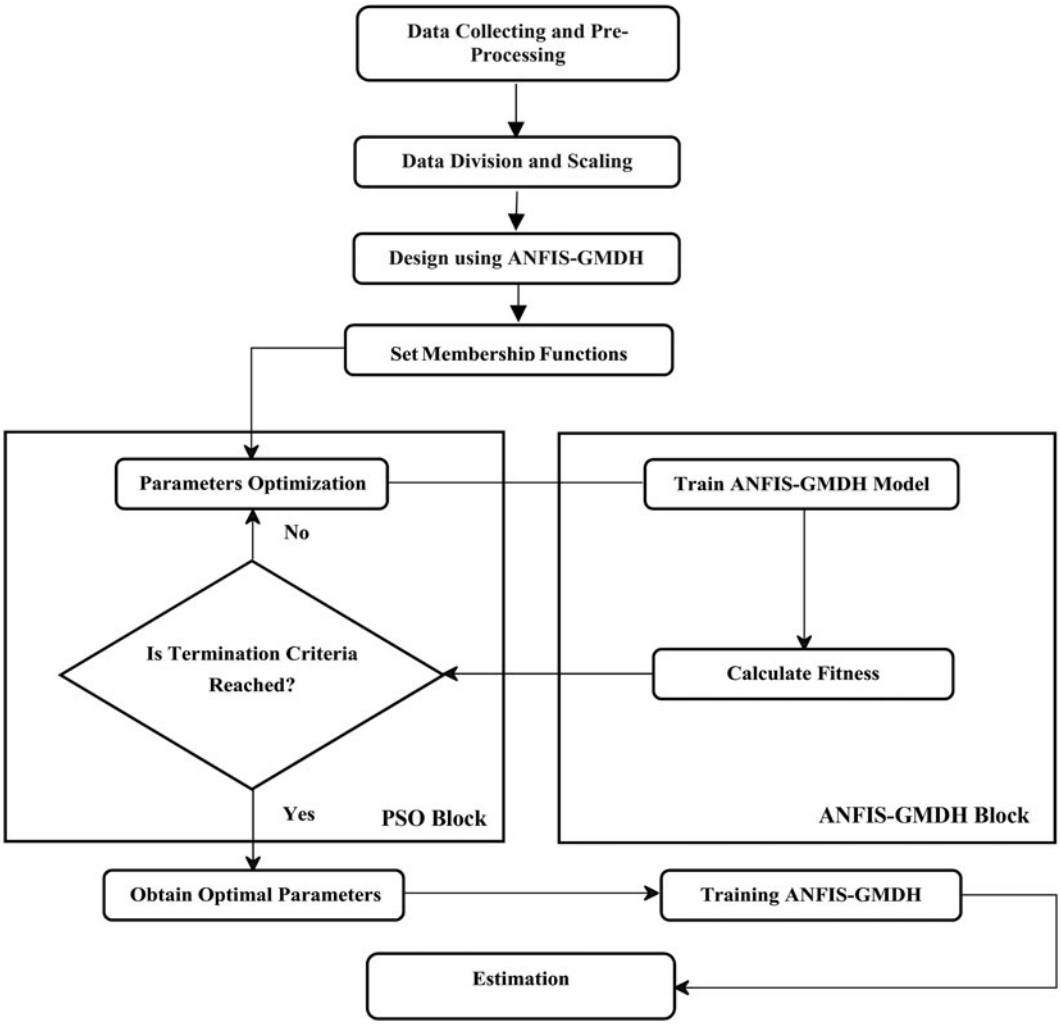


Fig. 4. Flowchart of the ANFIS-GMDH model optimized by the PSO algorithm.

Description of the PSO framework

The PSO technique is one of the metaheuristic algorithms inspired based on animals' swarm behavior presented by Eberhart and Kennedy (1995). The primary idea lies in simulating the social behavior of creatures such as birds and floating fish in a multidimensional space. In the PSO algorithm, the population size consists of a set of random individual particles (M) dispersed in a D-dimensional searching space (Eberhart and Kennedy, 1995).

Initially, to develop a PSO structure, a random position vector of $P^m = (P_1^m, P_2^m, \ldots, P_D^m)$ is defined for the data set domain and a vector of random velocity of $V^m = (V_1^m, V_2^m, \ldots, V_D^m)$ computed for $m = (1, 2, \ldots, M)$ in the interval of $[-V_{\max} + V_{\max}]$ for each particle. Each particle follows the two best vectors; one vector denoted as the best particle position as $P\text{best}^m = (P\text{best}_1^m, P\text{best}_2^m, \ldots, P\text{best}_D^m)$ that each particle experiences so far associated with the minimum cost function value. Another vector is denoted as the particle's best global position of $\text{Pbest}_g = (\text{Pbest}_{g1}, \text{Pbest}_{g2}, \ldots, \text{Pbest}_{gD})$ associated with the minimum cost function value obtained among the whole population. To find the optimal solution, position and velocity vectors of each particle are updated iteratively through Eqs (31) and (32) for their fly-experience in search space (Poli *et al.*, 2007).

$$V_d^m(t+1) = W \cdot V_d^m(t) + \phi_1 r_1(\text{Pbest}_d^m(t) - P_d^m(t)) + \phi_2 r_2(\text{Pbest}_{gd}(t) - P_d^m(t)), \quad (31)$$

$$P_d^m(t+1) = P_d^m(t) + V_d^m(t+1) \quad \text{for } m = 1, 2, \ldots, M, \quad d = 1, 2, \ldots, D, \quad (32)$$

in which W is the factor of inertia governing the effect of the previous velocity on the current velocity; and ϕ_1 and ϕ_2 denote the cognitive and social parameters, respectively, which control the velocity of the particles toward $\text{Pbest}^{(m)}$ and Pbest_g; r_1 and r_2 are generated random numbers in the interval [0, 1] and t represents the number of iterations (Najafzadeh *et al.*, 2015).

To stop swarm exploration and divergences, the velocity of all particles must be limited at intervals $[-V_{\max}, V_{\max}]$ in each repetition, where $V_{\max}$ relies on the maximum velocity that is allowed for particles. At higher values than $V_{\max}$, particles tend to go beyond the optimal solution, and in opposite cases, the particles are trapped in the local minima. The exploration mechanism of

https://doi.org/10.1017/S0890060420000025 Published online by Cambridge University Press

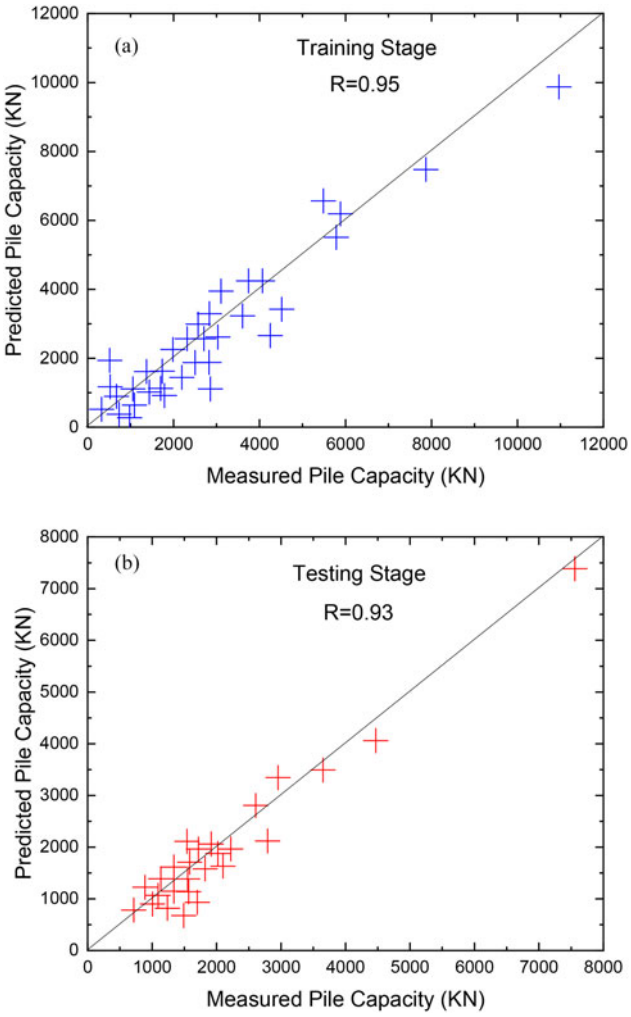


Fig. 5. Statistical and regression plot of the ANFIS-GMDH-PSO model in **(a)** training stage and **(b)** testing stage.

the optimization of particle swarm (PSO) is shown in Figure 1. The flowchart of the PSO algorithm is given in Figure 2.

Development of the hybrid ANFIS-GMDH-PSO algorithm

The PSO approach was applied for optimizing the ANFIS-GMDH structure and improving membership function parameters. Under such circumstances, the design of the ANFIS-GMDH involves the selection of fuzzy rules assigned higher firing strength (F_r). This selection causes to reduce the ANFIS-GMDH network error and number of selection rules. In the hybrid ANFIS-GMDH-PSO network model, a position vector (P^m) and velocity vector (V^m) were assigned for each particle in the following form:

$$P^m = (e_1^m, e_2^m, \ldots e_R^m, c_{11}^m, \ldots, c_{1K_1}^m, \ldots c_{nK_n}^m, \sigma_{11}^m, \ldots, \sigma_{1K_1}^m, \ldots, \sigma_{nK_n}^m, w_1^m, \ldots, w_R^m), \quad (33)$$

$$V^m = (V_1^m, V_2^m, \ldots, V_R^m, V_{R+1}^m, \ldots, V_z^m). \quad (34)$$

The $(e_1^m, e_2^m, \ldots, e_R^m)$ vector demonstrates the fuzzy rules effectiveness rate. Each e_r^m for $(r = 1, 2, \ldots, R)$ references to the connecting link between layer 3 and layer 4. In case the value of e_r^m is equal to one, it indicates that the relevant fuzzy inference rule is enabled, in other cases the fuzzy rule effect is ignored. It is noted that a fuzzy rule is preserved in terms of $\tilde{p}_r > \xi$ criteria (Fig. 3).

In which ξ denotes the amount of threshold specified by choice(i.e., $\xi = 5\%$) and $\tilde{p}_r$ is the pattern concentration percentage calculated as $\tilde{p}_r = (p_r/Q) \times 100(\%)$; in this relation, p_r indicates the number of patterns available in R^r with a firing strength of $F_r > 0.5$, and Q point outs to the number of training samples (Elloumi *et al.*, 2015).

The optimization problem was defined based on,

$$\text{Minimize fitness}\,(P^m) = \alpha \cdot F_1(P^m) + \beta \cdot \frac{1}{F_2(P^m)}. \quad (35)$$

The overall ANFIS network structure was described by a vector of $(e_1^m, e_2^m, \ldots, e_R^m)$. Therefore, the functions of F_1 and F_2 introduced through Eqs (36) and (37), respectively, are applied to P^m,

$$F_1(P^m) = 1 + \sum_{r=1}^{R} e_r^m, \quad (36)$$

$$F_2(P^m) = \frac{1}{(1/2) \cdot \sum_{q=1}^{Q} (\widehat{y}_q^m - y_q)^2} \quad (37)$$

where $\widehat{y}_q$ and y_q represent the adaptive neuro-fuzzy system output and observed target of the qth training sample.

The workflow of the developed ANFIS-GMDH-PSO flowchart is shown in Figure 4.

Table 2. Statistical analysis results in various applied methods for the test data set

Method	*R*	RMSE	MAE
Hybrid ANFIS-GMDH-PSO Model	0.93	336.90	271.31
Schmertmann	0.87	651.61	495.1
De Kuiter & Beringen	0.82	712.61	535.54
Bustamante & Gianeselli	0.85	670.89	554.76

Results and discussion

Hybrid ANFIS-GMDH-PSO model performance

Although several models can be derived from the hybrid ANFIS-GMDH-PSO model, the best fitted model must meet some statistical criteria prior to final model selection. From this perspective, a number of previously available statistical indices criterion have been presented by some researchers.

The precision level of these models was assessed by various statistical parameters. In this study, the coefficient of regression (R), root mean square error (RMSE), and mean absolute error (MAE) are

$$R = \frac{\sum_{i=1}^{n}(h_i - \bar{h})(t_i - \bar{t})}{\sqrt{\sum_{i=1}^{n}(h_i - \bar{h})^2 \sum_{i=1}^{n}(t_i - \bar{t})^2}}, \quad (38)$$

https://doi.org/10.1017/S0890060420000025 Published online by Cambridge University Press

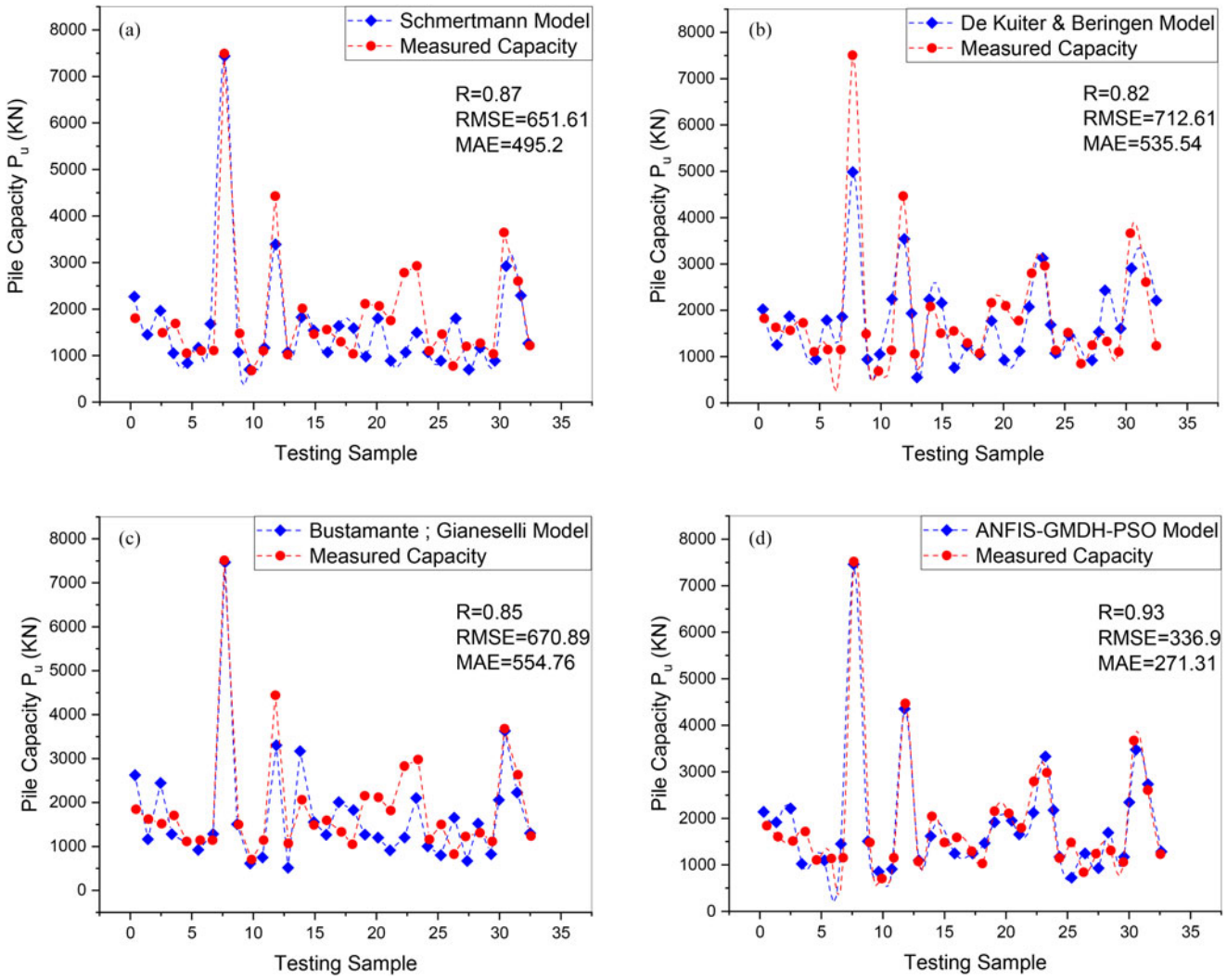


Fig. 6. Comparison of measured vs predicted values (P_u) by various methods for the testing data set.

$$\mathrm{RMSE} = \sqrt{\frac{\sum_{i=1}^{n} (h_i - t_i)^2}{n}}, \tag{39}$$

$$\mathrm{MAE} = \frac{1}{n} \sum_{i=1}^{n} |h_i - t_i|. \tag{40}$$

In the above-mentioned equations, h and t are the predicted P_u and observed P_u values, respectively. $\bar{h}$ and $\bar{t}$ represent the average value of predicted P_u and average P_u values obtained from measured pile loading test results (target values), respectively. These statistical criteria were frequently used to assess performance of various hybrid GMDH models in the field of the scouring process at hydraulic structures (e.g., Najafzadeh et al., 2013, 2015). From Eqs (38)–(40), it was observed that there are relatively good correlations between measured values (Observed Targets) and predicted values (model output) in cases where $R > 0.8$ or $R^2 > 0.64$, which indicates the perdition capability by proposed model.

It is noted that the sole use of R as the overall performance model's assessment is not normally sufficient to determine model precision since it is sensitive to the increase and relative variance between measured values and predicted values. Therefore, RMSE and MAE were also selected as auxiliary criteria in order to assess the accuracy level of the AI model. The best performance of AI is at the mercy of being zero in RMSE and MAE values. To display the ability of the ANFIS-GMDH-PSO model in pile bearing capacity prediction, the regression plot of measured values versus the predicted values is shown in Figure 5a,b for both training and testing stages.

From Table 2, it was found that the ANFIS-GMDH model has gained the highest R value and the lowest values of RMSE and MAE, estimating P_u in comparison with empirical equations. In addition, relatively close values of R, RMSE, and MAE in the training and testing data set showed that this AI model benefits from highly convincing performance. In order to ensure ANFIS-GMDH-PSO model performance, its predictability should be evaluated compared to empirical methods. In this regard, the same testing data set applied to the hybrid ANFIS-GMDH-PSO model was considered for comparing in various CPT-based methods. The results of the comparative analysis among different

https://doi.org/10.1017/S0890060420000025 Published online by Cambridge University Press

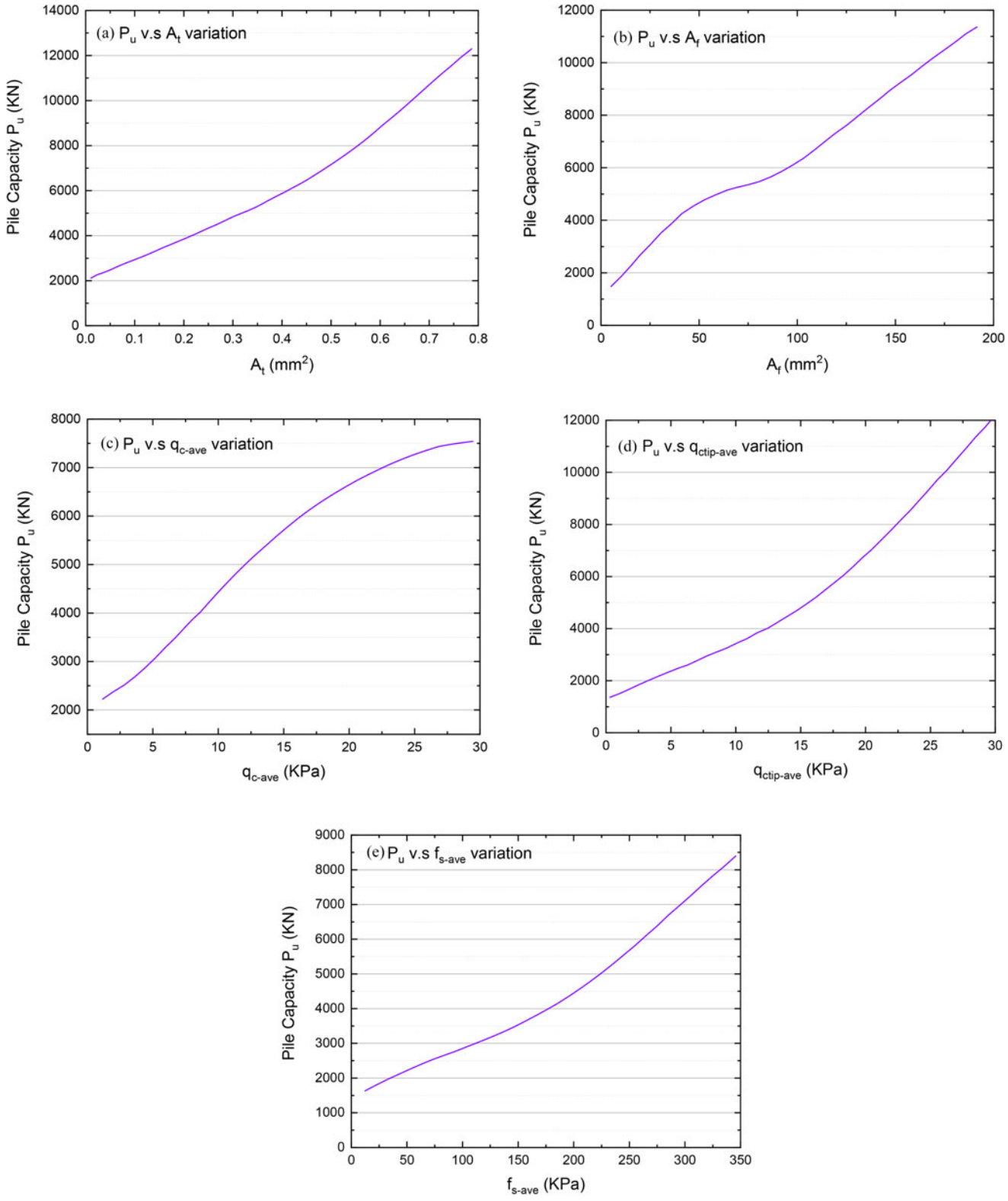


Fig. 7. Sensitivity analysis of the developed ANFIS-GMDH-PSO model for P_u prediction for **(a)** A_t variable variations, **(b)** A_s variable variations, **(c)** $\bar{q}_{c-shaft}$ variable variations, **(d)** $\bar{q}_{c-tip}$ variable variations, and **(e)** $\bar{f}_s$ variable variations.

models are shown in Figure 6. The values obtained from CPT-based methods are based on previous studies (Eslami, 1997; Kordjazi *et al.*, 2014).

The statistical parameters obtained from the developed network model (ANFIS-GMDH-PSO) are compared with those obtained by various empirical CPT-based models:

https://doi.org/10.1017/S0890060420000025 Published online by Cambridge University Press

Schmertmann (1978), De Kuiter and Beringen (1979), and Bustamante and Gianeselli (1982). Statistical results are presented in Table 2. To evaluate results obtained from the ANFIS-GMDH-PSO model and conventional methods, graphical results of empirical equations are shown in Figure 6 for calculating the UPBC.

Sensitivity analysis

Sensitivity analysis simulation was performed in this research to evaluate the prediction and validation ability of the developed ANFIS-GMDH-PSO model with the aid of statistical indices criterion in addition to comparing the results presented by some researchers through CPT-based models in this field.

Although the ANFIS-GMDH-PSO model showed that the developed model has a good enough approximation capability, it is necessary to consider the physical behavior of the model from an engineering perspective point view. For this purpose, the behavior and response of the model could be assessed based on individual various input variables and must compare with available empirical or theoretical approaches presented in previous studies.

Sensitivity analysis showed the response of the hybrid ANFIS-GMDH-PSO model to each variable variation. This task performed by changing only one input variable while the remaining input variables were kept constant in their average values; therefore, an artificial data set was designed for each one of the variables with respect to its range in the data source. Then input values are introduced to the proposed ANFIS-GMDH-PSO model and finally outputs were computed. This process was repeated using remaining one or more input variables until the model response is obtained for all predictive parameters. As shown in Figure 7, the results of the sensitivity analysis confirm the fact that the ANFIS-GMDH-PSO model predicted the P_u variable associated with physical behavior from an engineering perspective. It was shown that P_u values were increased with increasing $A_t, A_s, \bar{q}_{c-shaft}, \bar{q}_{c-tip}, \bar{f}_s$ values individually according to Figure 7.

Conclusion

In this study, two different neural networks including ANFIS and GMDH techniques were combined and optimized by the PSO method in order to develop hybrid ANFIS-GMDH-PSO for predicting bearing capacity of driven piles. In this way, 108 data sets in the form of an input–output system were composed of six input variables including both coarse and fine grain soils, cone tip resistance and sleeve friction of CPTs, and geometric characterizations of piles. In the first step, the general hybrid structure of the ANFIS-GMDH model was developed and optimized using PSO. Furthermore, in the second step, three well-known empirical equations were used for comparison with the proposed AI model. The effective input parameters were involved and selected including pile and soil characteristics, PLT, and CPT results during the developed proposed model.

Comparison of the achieved results with the actual target data set showed that the hybrid ANFIS-GMDH-PSO algorithm displayed proper desired output in predicting the pile bearing capacity. In addition, this developed model showed a better performance and relative proper accuracy compared to other empirical methods established based on the CPT. The ANFIS-GMDH-PSO model does not suffer in local optimal traps by applying the PSO algorithm, and it also increases the accuracy and global search capability for ANFIS-GMDH-PSO training. This research emphasized the ability of AI-based methods to provide some more accurate methods than other analytical and empirical methods. Statistical results demonstrated that the ANFIS-GMDH-PSO models have provided better performance than other mentioned empirical CPT-based methods. Besides, results of sensitivity analysis showed that the diameter of driven pile (D) and sleeve friction (f_s) parameters had the highest and lowest impacts on the bearing capacity of driven pile. Generally, performance of the integrated model of ANFIS-GMDH indicated that this soft computing tool can be employed efficiently to solve one of the most important issues in geotechnical engineering.

References

Abu-Farsakh MY and Titi HH (2004) Assessment of direct cone penetration test methods for predicting the ultimate capacity of friction driven piles. *Journal of Geotechnical and Geoenvironmental Engineering* **130**, 935–944.

Abu-Kiefa M (1998) General regression neural networks for driven piles in cohesionless soils. *Journal of Geotechnical and Geoenvironmental Engineering* **124**, 1177–1185.

Adeniran AA and El-Ferik S (2017) A reinforced combinatorial particle swarm optimization based multimodel identification of nonlinear systems. *Artificial Intelligence for Engineering Design, Analysis and Manufacturing* **31**, 327–358.

Alkroosh IS and Nikraz H (2011) Correlation of pile axial capacity and CPT data using gene expression programming. *Geotechnical and Geological Engineering* **29**, 725–748.

Alkroosh IS and Nikraz H (2012) Predicting axial capacity of driven piles in cohesive soils usingintelligent computing. *Engineering Applications of Artificial Intelligence* **25**, 618–627.

Al-Refaie A, Judeh M and Li M-H (2018) Optimal fuzzy scheduling and sequencing of multiple-period operating room. *Artificial Intelligence for Engineering Design, Analysis and Manufacturing* **32**, 108–121.

Armaghani DJ, Raja RSNSB, Faizi K and Rashid ASA (2017) Developing a hybrid PSO–ANN model for estimating the ultimate bearing capacity of rock-socketed piles. *Neural Computing and Applications* **28**, 391–405.

Armaghani DJ, Faradonbeh RS, Rezaei H, Rashid ASA and Amnieh HB (2018) Settlement prediction of the rock-socketed piles through a new technique based on gene expression programming. *Neural Computing and Applications* **29**, 1115–1125.

Begemann HP (1963) The use of the static soil penetrometer in Holland. *New Zealand Engineering* **18**.

Bustamante M and Gianeselli L (1982) Pile bearing capacity prediction by means of static penetrometer CPT. In *Proceedings of the 2-nd European symposium on penetration testing*, pp. 493–500.

Coello CAC and Aguirre AH (2002) Design of combinational logic circuits through an evolutionary multiobjective optimization approach. *Artificial Intelligence for Engineering Design, Analysis and Manufacturing* **16**, 39–53.

De Kuiter J and Beringen F (1979) Pile foundations for large North Sea structures. *Marine Georesources & Geotechnology* **3**, 267–314.

Eberhart R and Kennedy J (1995) A new optimizer using particle swarm theory. In *MHS'95. Proceedings of the Sixth International Symposium on Micro Machine and Human Science*, 4–6 Oct, IEEE, Nagoya, Japan, pp. 39–43. DOI: 10.1109/MHS.1995.494215.

Ebrahimian B and Movahed V (2016) Application of an evolutionary-based approach in evaluating pile bearing capacity using CPT results. *Ships and Offshore Structures* **12**, 1–17.

Elloumi M, Krid M and Masmoudi DS (2015) Neuro-fuzzy system based on particle swarm optimization algorithm for image denoising application. *Paper presented at the Advances in Biomedical Engineering (ICABME), 2015 International Conference on.*

Eslami A (1997) *Bearing Capacity of Piles From Cone Penetration Test Data*. Canada: University of Ottawa.

https://doi.org/10.1017/S0890060420000025 Published online by Cambridge University Press

Faizi K, Armaghani DJ, Sohaei H, Rashid ASA and Nazir R (2015) Deformation model of sand around short piles under pullout test. *Measurement* **63**, 110–119.

Hanna S (2007) Inductive machine learning of optimal modular structures: estimating solutions using support vector machines. *Artificial Intelligence for Engineering Design, Analysis and Manufacturing* **21**, 351–366.

Harandizadeh H, Toufigh MM and Toufigh V (2018) Application of improved ANFIS approaches to estimate bearing capacity of piles. *Soft Computing* **23**, 1–13.

Haykin S, Nie J and Currie B (1999) Neural network-based receiver for wireless communications. *Electronics Letters* **35**, 203–205.

Hu Y-J, Wang Y, Wang Z-L, Wang Y-Q and Zhang B-C (2014) Machining scheme selection based on a new discrete particle swarm optimization and analytic hierarchy process. *Artificial Intelligence for Engineering Design, Analysis and Manufacturing* **28**, 71–82.

Kalantary F, Ardalan H and Nariman-Zadeh N (2009) An investigation on the Su–NSPT correlation using GMDH type neural networks and genetic algorithms. *Engineering Geology* **104**, 144–155.

Keles HY (2018) Embedding parts in shape grammars using a parallel particle swarm optimization method on graphics processing units. *Artificial Intelligence for Engineering Design, Analysis and Manufacturing* **32**, 256–268.

Kennedy J and Eberhart R (1995) Perth, Australia. In *Proc. IEEE International Conference on Neural Networks*.

Kiefa MA (1998) General regression neural networks for driven piles in cohesionless soils. *Journal of Geotechnical and Geoenvironmental Engineering* **124**, 1177–1185.

Kondner RL (1963) Hyperbolic stress-strain response: cohesive soils. *Journal of the Soil Mechanics and Foundations Division* **89**, 115–144.

Kontovourkis O, Phocas MC and Lamprou I (2015) Adaptive kinetic structural behavior through machine learning: optimizing the process of kinematic transformation using artificial neural networks. *Artificial Intelligence for Engineering Design, Analysis and Manufacturing* **29**, 371–391.

Koopialipoor M, Nikouei SS, Marto A, Fahimifar A, Jahed Armaghani D and Mohamad ET (2018) Predicting tunnel boring machine performance through a new model based on the group method of data handling. *Bulletin of Engineering Geology and the Environment* **78**, 1–14.

Kordjazi A, Nejad FP and Jaksa M (2014) Prediction of ultimate axial load-carrying capacity of piles using a support vector machine based on CPT data. *Computers and Geotechnics* **55**, 91–102.

Lin C-J and Huang M-L (2018) Efficient hybrid group search optimizer for assembling printed circuit boards. *Artificial Intelligence for Engineering Design, Analysis and Manufacturing*, 1–16. doi:10.1017/S0890060418000240

Mirabi M and Seddighi P (2018) Hybrid ant colony optimization for capacitated multiple-allocation cluster hub location problem. *Artificial Intelligence for Engineering Design, Analysis and Manufacturing* **32**, 44–58.

Moayedi H and Armaghani DJ (2018) Optimizing an ANN model with ICA for estimating bearing capacity of driven pile in cohesionless soil. *Engineering with Computers* **34**, 347–356.

Mola-Abasi H and Eslami A (2018) Prediction of drained soil shear strength parameters of marine deposit from CPTu data using GMDH-type neural network. *Marine Georesources and Geotechnology* **37**, 1–10.

Momeni E, Nazir R, Jahed Armaghani D and Maizir H (2014) Prediction of pile bearing capacity using a hybrid genetic algorithm-based ANN. *Measurement* **57**, 122–131.

Momeni E, Nazir R, Armaghani DJ and Maizir H (2015) Application of artificial neural network for predicting shaft and tip resistances of concrete piles. *Earth Sciences Research Journal* **19**, 85–93.

Momeni E, Armaghani DJ, Fatemi SA and Nazir R (2018) Prediction of bearing capacity of thin-walled foundation: a simulation approach. *Engineering with Computers* **34**, 319–327.

Naeinia SA, Ziaie Moayeda R, Kordnaeija A and Mola-Abasib H (2018) Elasticity modulus of clayey deposits estimation using Group Method of Data Handling type neural network. *Measurement* **121**, 335–343.

Najafzadeh M (2015) Neuro-fuzzy GMDH based evolutionary algorithms to predict the scour pile under clear-water condition. *Ocean Engineering* **99**, 85–94.

Najafzadeh M and Azamathulla HM (2013) Neuro-fuzzy GMDH systems to predict the scour pile groups due to waves. *Journal of Computing in Civil Engineering*. doi:10.1061/(ASCE)CP.1943-5487.0000376.

Najafzadeh M and Barani GA (2011) Comparison of group method of data handling based genetic programming and back propagation systems to predict scour depth around bridge piers. *Scientia Iranica Transactions A: Civil Engineering* **18**, 1207–1213.

Najafzadeh M and Lim S-Y (2015) Application of improved neuro-fuzzy GMDH to predict scour downstream of sluice gates. *Earth Science Informatics* **8**, 187–196.

Najafzadeh M and Saberi-Movahed F (2019) GMDH-GEP to predict free span expansion rates below pipelines under waves. *Marine Georesources & Geotechnology* **37**, 375–392.

Najafzadeh M and Tafarojnoruz A (2016) Neuro-fuzzy GMDH based particle swarm optimization to predict longitudinal dispersion coefficients in rivers. *Environmental Earth Sciences* **75**, 1–16.

Najafzadeh M, Barani GA and Azamathulla HM (2013a) GMDH to predict scour depth around a pier in cohesive soils. *Applied Ocean Research*.**40**, 35–41.

Najafzadeh M, Barani GA and Hessami-Kermani MR (2013b) Group method of data handling to predict scour depth around vertical piles under regular waves. *Scientia Iranica* **20**(3), 406–413.

Najafzadeh M, Barani GA and Azamathulla HM (2014) Prediction of pipeline scour depth in clear-water and live-bed conditions using GMDH. *Neural Computing and Applications* **24**, 629–635.

Najafzadeh M, Barani GA and Hessami-Kermani MR (2015) Evaluation of GMDH networks for prediction of local scour depth at bridge abutments in coarse sediments with thinly armored beds. *Ocean Engineering* **104**, 387–396.

Najafzadeh M, Saberi-Movahed F and Sarkamaryan S (2018) NF-GMDH-Based self-organized systems to predict bridge pier scour depth under debris flow effects. *Marine Georesources and Geotechnology* **36**, 589–602.

Nariman-Zadeh N, Darvizeh A and Dadfarmai MH (2003) Adaptive neuro-fuzzy inference systems networks design using hybrid genetic and singular value decomposition methods for modeling and prediction of the explosive cutting process. *Artificial Intelligence for Engineering Design Analysis and Manufacturing* **17**, 313–324.

Nejad FP, Jaksa MB, Kakhi M and McCabe BA (2009) Prediction of pile settlement using artificial neural networks based on standard penetration test data. *Computers and Geotechnics* **36**, 1125–1133.

Niazi FS and Mayne PW (2013) Cone penetration test based direct methods for evaluating static axial capacity of single piles. *Geotechnical and Geological Engineering* **31**, 979–1009.

Padmini D, Ilamparuthi K and Sudheer K (2008) Ultimate bearing capacity prediction of shallow foundations on cohesionless soils using neurofuzzy models. *Computers and Geotechnics* **35**, 33–46.

Persson JA and Ölvander J (2017) How to compare performance of robust design optimization algorithms, including a novel method. *Artificial Intelligence for Engineering Design, Analysis and Manufacturing* **31**, 286–297.

Poli R, Kennedy J and Blackwell T (2007) Particle swarm optimization. *Swarm intelligence* **1**, 33–57.

Rossi A and Lanzetta M (2013) Non-permutation flow line scheduling by ant colony optimization. *Artificial Intelligence for Engineering Design, Analysis and Manufacturing* **27**, 349–357.

Salido MA, Escamilla J, Barber F, Giret A, Tang D and Dai M (2015) Energy efficiency, robustness, and make span optimality in job-shop scheduling problems. *Artificial Intelligence for Engineering Design, Analysis and Manufacturing* **30**, 300–312.

Schmertmann JH (1978) Guidelines for cone penetration test: performance and design. United States. Federal Highway Administration. Office of Research and Development https://rosap.ntl.bts.gov/view/dot/958.

Shaghaghi S, Bonakdari H, Gholami A, Ebtehaj I and Zeinolabedini M (2017) Comparative analysis of GMDH neural network based on genetic algorithm and particle swarm optimization in stable channel design. *Applied Mathematics and Computation* **313**, 271–286.

Shahin MA (2010) Intelligent computing for modeling axial capacity of pile foundations. *Canadian Geotechnical Journal* **47**, 230–243.

Takagi T and Sugeno M (1993) A fuzzy logic approach to qualitative modelling. *IEEE Trans. Fuzzy Systems* **1**, 7–31

https://doi.org/10.1017/S0890060420000025 Published online by Cambridge University Press

Thimmisetty C, Tsilifis P and Ghanem R (2017) Homogeneous chaos basis adaptation for design optimization under uncertainty: application to the oil well placement problem. *Artificial Intelligence for Engineering, Design Analysis and Manufacturing* **31**, 265–276.

Zadeh LA (1996) In *Fuzzy Sets, Fuzzy Logic, And Fuzzy Systems*. Binghamton, New york, USA: Binghamton University-SUNY, pp. 394–432.

Zeng K, Tan Z, Dong M and Yang P (2014) Probability increment based swarm optimization for combinatorial optimization with application to printed circuit board assembly. *Artificial Intelligence for Engineering Design, Analysis and Manufacturing* **28**, 429–437.

Zhang Z, Ding D, Rao L and Bi Z (2006) An ANFIS based approach for predicting the ultimate bearing capacity of single piles. In *Foundation Analysis and Design: Innovative Methods*, pp. 159–166

Zimmermann L, Chen T and Shea K (2018) A 3D, performance-driven generative design framework: automating the link from a 3D spatial grammar interpreter to structural finite element analysis and stochastic optimization. *Artificial Intelligence for Engineering Design, Analysis and Manufacturing* **32**, 189–199.

Dr Hooman Harandizadeh He graduated and received his Ph. D degree in Geotechnical Engineering from Shahid Bahonar University of Kerman, Iran in 2018 and he also received his MS. CE in Structural and Geotechnical Engineering from University of San Carlos, Philippine in 2010. His main interested research areas include soil and rock mechanics, pile foundation analysis and design, slope stability, soft computing modelling, and artificial intelligence methods. He has published some papers in various journals with ISI indexing. He is also reviewer of Civil engineering and AI & soft computing journals.

https://doi.org/10.1017/S0890060420000025 Published online by Cambridge University Press